
Article:
Zhao, X, Barber, S orcid.org/0000-0002-7611-7219, Taylor, CC orcid.org/0000-0003-0181-1094 et al. (1 more author) (2018) Classification tree methods for panel data using wavelet-transformed time series. Computational Statistics and Data Analysis, 127. pp. 204-216. ISSN 0167-9473

https://doi.org/10.1016/j.csda.2018.05.019

Classification tree methods for panel data using wavelet-transformed time series

Xin Zhao[a], Stuart Barber[a1], Charles C Taylor[a], Zoka Milan[b]

[a] *School of Mathematics, University of Leeds, U.K.*
[b] *King's College Hospital Trust, London, U.K.*

Abstract

Wavelet-transformed variables can have better classification performance for panel data than using variables on their original scale. Examples are provided showing the types of data where using a wavelet-based representation is likely to improve classification accuracy. Results show that in most cases wavelet-transformed data have better or similar classification accuracy to the original data, and only select genuinely useful explanatory variables. Use of wavelet-transformed data provides localized mean and difference variables which can be more effective than the original variables, provide a means of separating "signal" from "noise", and bring the opportunity for improved interpretation via the consideration of which resolution scales are the most informative. Panel data with multiple observations on each individual require some form of aggregation to classify at the individual level. Three different aggregation schemes are presented and compared using simulated data and real data gathered during liver transplantation. Methods based on aggregating individual level data before classification outperform methods which rely solely on the combining of time-point classifications.

Keywords: CART, MODWT, panel data, noise exclusion

1. Introduction

We often encounter data containing multiple time series variables for organisations or individuals that need classification, especially in areas such as economics, finance, marketing, medicine and biology. It can also be important to determine which of the time series are useful in performing the classification; interpreting this

[1]School of Mathematics, University of Leeds, Leeds LS2 9JT, UK. Email S.Barber@leeds.ac.uk

information can be highly useful in investigating the relationships between the variables and the class labels.

Our interest in this problem was motivated by data collected on patients undergoing liver transplant surgery. Each patient is classified into one of two groups, according to whether they did or did not use beta-blocker medication. During the operation, monitoring took place for several variables such as heart rate and systolic blood pressure, with data recorded once every heartbeat. However, equivalent problems arise in many different contexts.

Denote the data as $A_{n,k,t}$ for individual (or organisation) $n = 1, 2, \ldots, N$, variable $k = 1, 2, \ldots, K$, and time $t = 1, 2, \ldots, T_n$, allowing the length of the time series to be different for each individual. Thus, for the n^{th} individual, the data can be expressed as a $T_n \times K$ matrix

$$A_{n,\cdot,\cdot} = \begin{bmatrix} A_{n,1,1} & \cdots & A_{n,K,1} \\ A_{n,1,2} & \cdots & A_{n,K,2} \\ \vdots & \ddots & \vdots \\ A_{n,1,T_n} & \cdots & A_{n,K,T_n} \end{bmatrix}.$$

The full data can be written as a $\sum_{n=1}^{N} T_n \times K$ matrix A, where

$$A^T = \begin{bmatrix} A^T_{1,\cdot,\cdot} & A^T_{2,\cdot,\cdot} & \cdots & A^T_{N,\cdot,\cdot} \end{bmatrix}.$$

We refer to such explanatory data as panel (or longitudinal) data. The response variable Y is the group that each individual belongs to, which we write as a vector

$$y^T = \begin{bmatrix} y^T_{1,\cdot} & y^T_{2,\cdot} & \cdots & y^T_{N,\cdot} \end{bmatrix},$$

where $y_{n,\cdot}$ has T_n identical values, defined by $(y_{n,1}, y_{n,2}, \ldots, y_{n,T_n})$.

Difficulties in analysing such datasets include: (1) unequal values of T_n; (2) aggregating the panel data to provide classification for each individual; and (3) lack of independence between consecutive times.

Such data are generally subject to noise if they are collected or recorded by people or machines. Wavelet shrinkage (Donoho and Johnstone, 1994) is a popular denoising method, which is commonly used to smooth out random noise variation in signals, and we could use such methods in our application. However, even without a formal denoising step, wavelets are able to separate out "signal" from "noise", and we use this property to improve prediction performance. We shall also see that wavelets can pick out short term fluctuations in real data which can be exploited for classification when consecutive observations lack independence. Instead of using the standard

decimated discrete wavelet transform (DWT), we use the maximal overlap discrete wavelet transform (MODWT; see, for example, Percival and Walden (2000, ch. 5)), as it is not constrained by time series length T_n and each time point is represented at all resolution levels of the MODWT. Equivalent translation-equivariant transforms are the non-decimated stationary wavelet transform (Nason and Silverman, 1995) and cycle-spinning (Coifman and Donoho, 1995).

For classification, we use the classification and regression tree (CART) method of Breiman et al. (1984). Using DWT (or MODWT) with CART (or other decision trees or random forests) in time series data has already been considered (Alickovic and Subasi, 2016; Gokgoz and Subasi, 2015; Upadhyaya and Mohanty, 2016), as have other classification methods (Maharaj and Alonso, 2007, 2014) but, to the best of our knowledge, until now the application to panel data is quite rare. Previous authors have directly converted the wavelet representation of panel data into cross-sectional data by using summaries such as energy, standard deviation, or entropy (Zhang et al., 2015; Upadhyaya and Mohanty, 2016).

However detecting when and how MODWT can help CART in classification accuracy and variable selection for panel data is important. Thus, in this paper, we use CART with original and wavelet-transformed variables to classify panel data. We introduce our methodology in Section 2, and apply it to simulated panel data experiments in Section 3 before analysing our liver transplantation (LT) panel data in Section 4. Some concluding comments appear in Section 5.

2. Methodology

In this section, CART and the MODWT are introduced briefly. For more details, see Breiman et al. (1984) and Percival and Walden (2000), respectively. We then propose three methods to produce individual-level classifications from panel data, which can be applied to the original data, the wavelet-transformed data, or a combination of both.

2.1. Background

The goal of CART is to construct a model that predicts the value of a response variable by learning simple decision rules inferred from data features. In our case, we use classification trees since the response variable is categorical. The model built is structured as a tree with each node representing a split of the data in that node according to the value of a single variable. The aim is to use successive decision rules to split the data in a way which makes the subset of data at each terminal node (leaf node) as pure as possible, ideally with only one class. The tree represents, therefore,

a classification rule using only those variables which are found to convey as much relevant information as possible. The tree construction process involves building and then pruning a tree. In the tree building process, we use optimization of the Gini index as our splitting criterion to choose the best explanatory variable to construct a decision at each node. Specifically, the decision rule using the selected variable at each node will determine a subset of the data which is as pure as possible, as measured by the Gini index. In the pruning process, we use ten-fold cross-validation to mitigate the tendency of CART to produce over-fitted models. Overall, then, CART is used to construct a classification rule which incorporates a variable selection stage as part of the construction process.

In the MODWT, we use the Haar scaling function ϕ and wavelet ψ, where

$$\phi(\tau) = \begin{cases} 1 & \tau \in [0,1) \\ 0 & \text{else,} \end{cases} \qquad \text{and} \qquad \psi(\tau) = \begin{cases} 1 & \tau \in [0,1/2) \\ -1 & \tau \in [1/2,1) \\ 0 & \text{else.} \end{cases} \tag{1}$$

By using dilation and translation, we obtain the scaling function and wavelet at location l and resolution level j:

$$\phi_{j,l}(\tau) = 2^{j/2}\phi\big(2^j(\tau - l)\big) \qquad \text{and} \qquad \psi_{j,l}(\tau) = 2^{j/2}\psi\big(2^j(\tau - l)\big),$$

where $j = 0, 1, \ldots, J$, for $J = \lfloor \log_2 n \rfloor$, and $l = 0, 1, \ldots, n-1$. Note that $\phi_{j,l}$ and $\psi_{j,l}$ are compactly supported on $I_{j,l} = \big[2^{-j}l, 2^{-j}(l+1)\big)$. When $j = 0$, the scaling coefficients are actually the original time series values.

To represent our data in terms of the Haar wavelet basis, we compute scaling coefficients $s_{j,l}$ defined by

$$s_{j,l} = \langle A_{n,k,.}, \phi_{j,l} \rangle = \sum_{t=1}^{T_n} A_{n,k,t}\phi_{j,l}(t/T_n) = 2^{j/2} \sum_{t/T_n \in I_{j,l}} A_{n,l,t}.$$

The Haar wavelet coefficients $d_{j,k}$ can then be calculated as $d_{j,l} = s_{j-1,l} - s_{j,l}$; hence coefficients of $\phi_{j,l}$ and $\psi_{j,l}$ represent local averages and contrasts, respectively, in the interval $I_{j,l}$. To interpret these coefficients, note that when j is small the corresponding scaling and wavelet functions are highly localized at that fine scale, representing brief transient effects. Conversely, when j is large, they represent lower frequency activity at a coarser scale.

The scaling coefficients s and wavelet coefficients d are treated as new variables which we can use for classification. We denote the wavelet transformed data

MODWT($A_{n,k,\cdot}$) for variable k on individual n as the $T_n \times 2J$ matrix $W_{n,k,\cdot}$, where

$$W_{n,k,\cdot} = \left[\begin{array}{ccc|ccc} W^{d_1}_{n,k,1} & \cdots & W^{d_j}_{n,k,1} & W^{s_1}_{n,k,1} & \cdots & W^{s_j}_{n,k,1} \\ W^{d_1}_{n,k,2} & \cdots & W^{d_j}_{n,k,2} & W^{s_1}_{n,k,2} & \cdots & W^{s_j}_{n,k,2} \\ \vdots & \ddots & \vdots & \vdots & \ddots & \vdots \\ W^{d_1}_{n,k,T_n} & \cdots & W^{d_j}_{n,k,T_n} & W^{s_1}_{n,k,T_n} & \cdots & W^{s_j}_{n,k,T_n} \end{array}\right].$$

The wavelet transformed explanatory data are then

$$W = \left[\begin{array}{ccc} W_{1,1,\cdot} & \cdots & W_{1,K,\cdot} \\ W_{2,1,\cdot} & \cdots & W_{2,K,\cdot} \\ \vdots & \ddots & \vdots \\ W_{N,1,\cdot} & \cdots & W_{N,K,\cdot} \end{array}\right].$$

2.2. Classification methods

Since we wish to classify individuals, but are dealing with panel data, we can not use the predictions from CART directly as these classify each time point separately. We need to combine the information either by combining time-point level predictions or aggregating data first and then performing classification for individuals. We now propose several methods to classify individuals based on panel data, which we illustrate in terms of the original data A. Equivalently, these methods can also be applied to the wavelet-transformed data W, or indeed to a combination of A and W. For simplicity, each of the methods is described in terms of a binary classification, but is easily generalized to more than two groups.

2.2.1. Method 1: prediction aggregation after classification

Using CART, we can obtain the predicted class $\hat{y}_{n,t}$ of each individual for every time point $t = 1, \ldots, T_n$ and schematically we have

$$A_{n,\cdot,\cdot} = \left[\begin{array}{ccc} A_{n,1,1} & \cdots & A_{n,K,1} \\ A_{n,1,2} & \cdots & A_{n,K,2} \\ \vdots & \ddots & \vdots \\ A_{n,1,T_n} & \cdots & A_{n,K,T_n} \end{array}\right] \rightarrow \hat{y}_{n,\cdot} = \left[\begin{array}{c} \hat{y}_{n,1} \\ \hat{y}_{n,2} \\ \vdots \\ \hat{y}_{n,T_n} \end{array}\right].$$

For individual n, we compute the proportion of time points which were classified as group 1,

$$P_n = \frac{1}{T_n} \sum_{t=1}^{T_n} I\{\hat{y}_{n,t} = 1\},$$

where we define the indicator variable

$$I\{\hat{y}_{n,t} = 1\} = \begin{cases} 1 & \text{if } \hat{y}_{n,t} = 1 \\ 0 & \text{if } \hat{y}_{n,t} = 2. \end{cases}$$

We use the prediction at each time point to predict the class of individual n:

$$A_{n,\cdot,\cdot} \to \hat{y}_n = \begin{cases} 1 & \text{if } P_n \geqslant a \\ 2 & \text{otherwise,} \end{cases}$$

where the best split point a is found by using a global search.

2.2.2. Method 2: predictions based on time-point level and individual level CART

Here, we first construct a classification tree as in Method 1. Variable k' is used in this classification tree, where $k' \in \{1, 2, \ldots, K'\}$, making a total of K' newly renumbered variables. So the data set used in this tree becomes

$$A'_{n,\cdot,\cdot} = [A_{n,k',t}]_{T_n \times K'}.$$

For each observed value of each of these variables, we first use the tree to derive the probability of classifying an observation as being from group 1, based on the subtree descending from that observation.

Consider variable k'. To compute the derived probabilities, we inspect the nodes in the tree where variable k' is used. In a node, with split point η, observations satisfying $A_{n,k',t} < \eta$ are directed to one sub-tree, while those satisfying $A_{n,k',t} > \eta$ are directed to a different sub-tree. In each sub-tree, we find the proportion classified as group 1, and replace $A_{n,k',t}$ by this probability, which we denote as $P_{n,k',t}$.

For example, for $A_{n,k',t}$, if $A_{n,k',t} > \eta$, then

$$P_{n,k',t} = P_{A_{n,k',\cdot} > \eta},$$

where $P_{A_{n,k',\cdot} > \eta}$ is the proportion classified as group 1 for variable k' in that sub node satisfying $A_{n,k',\cdot} > \eta$.

If variable k' is used in more than one node, we take the product of the probabilities (note that $k' \in \{1, 2, \ldots, K'\}$ implies that variable k' must be used in at least one node). For example, if variable k' appeared twice, with thresholds η_1 and η_2, then

$$P_{n,k',t} = P_{A_{n,k',\cdot} > \eta_1} \cdot P_{A_{n,k',\cdot} > \eta_2},$$

where $P_{A_{n,k',\cdot} > \eta_1}$ and $P_{A_{n,k',\cdot} > \eta_2}$ are the proportions classified as group 1 for variable k' in the nodes satisfying $A_{n,k',\cdot} > \eta_1$ and $A_{n,k',\cdot} > \eta_2$ respectively.

This whole process is repeated for each $k' \in \{1, 2, \ldots, K'\}$ in turn, converting each time series of observed values to a vector of proportions and finally, from $A'_{n,.,.}$, we get

$$P_{n,.,.} = [P_{n,k',t}]_{K' \times T_n}.$$

Then we take the mean and standard deviation of these empirical probabilities as new variables to use in a "second-stage" CART. (Of course, other summaries could be used.) Schematically, we have

$$P_{n,\cdot,\cdot} = \begin{bmatrix} P_{n,1,1} & \cdots & P_{n,K',1} \\ P_{n,1,2} & \cdots & P_{n,K',2} \\ \vdots & \ddots & \vdots \\ P_{n,1,T_n} & \cdots & P_{n,K',T_n} \end{bmatrix} \tag{2}$$

$$\swarrow\searrow \qquad\qquad \swarrow\searrow$$

$$P^{(m)}_{n,k,.} = \begin{bmatrix} P^{(m)}_{n,1,.}, P^{(sd)}_{n,1,.} & \cdots & P^{(m)}_{n,K',.}, P^{(sd)}_{n,1,.} \end{bmatrix}.$$

We then calculate the mean and standard deviation matrix for all individuals and variables as a cross sectional data

$$\widetilde{P} = \left[\begin{array}{ccc|ccc} P^{(m)}_{1,1,.} & \cdots & P^{(m)}_{1,K',.} & P^{(sd)}_{1,1,.} & \cdots & P^{(sd)}_{1,K',.} \\ P^{(m)}_{2,1,.} & \cdots & P^{(m)}_{2,K',.} & P^{(sd)}_{2,1,.} & \cdots & P^{(sd)}_{2,K',.} \\ \vdots & \ddots & \vdots & \vdots & \ddots & \vdots \\ P^{(m)}_{N,1,.} & \cdots & P^{(m)}_{N,K',.} & P^{(sd)}_{N,1,.} & \cdots & P^{(sd)}_{N,K',.} \end{array}\right]. \tag{3}$$

After that, we apply CART to $\widetilde{P}$, and get the predicted value for each individual:

$$\widetilde{P} = \left[\begin{array}{ccc|ccc} P^{(m)}_{1,1,.} & \cdots & P^{(m)}_{1,K',.} & P^{(sd)}_{1,1,.} & \cdots & P^{(sd)}_{1,K',.} \\ P^{(m)}_{2,1,.} & \cdots & P^{(m)}_{2,K',.} & P^{(sd)}_{2,1,.} & \cdots & P^{(sd)}_{2,K',.} \\ \vdots & \ddots & \vdots & \vdots & \ddots & \vdots \\ P^{(m)}_{N,1,.} & \cdots & P^{(m)}_{N,K',.} & P^{(sd)}_{N,1,.} & \cdots & P^{(sd)}_{N,K',.} \end{array}\right] \rightarrow \hat{y} = \begin{bmatrix} \hat{y}_1 \\ \hat{y}_2 \\ \vdots \\ \hat{y}_N \end{bmatrix}. \tag{4}$$

Note that in this second stage, each individual has just one mean and one standard deviation value corresponding to each of the variables in that tree, hence there is only one predicted class for each individual.

2.2.3. Method 3: data aggregation before classification

Here, we aggregate the original data for each individual into a small number of summaries for each variable — chosen to reflect the nature of the data — to form

individual level cross-sectional data, and then use CART directly. In our implementation, we use the mean $A^{(m)}_{n,k,\cdot}$ and standard deviation $A^{(sd)}_{n,k,\cdot}$ of variable k for each individual n $A_{n,k,t}$ to construct cross sectional data

$$\widetilde{A} = [A^{(m)},\, A^{(sd)}]_{N\times 2K},$$

where $A^{(m)} = [\, A^{(m)}_{n,k,\cdot}\,]_{N\times K}$ and $A^{(sd)} = [\, A^{(sd)}_{n,k,\cdot}\,]_{N\times K}$. The process is the same as in Equations (2) to (4), but applied to data A rather than probabilities P.

3. Simulation study

We now explore the performance of Methods 1–3 using both original and wavelet-transformed data in a simulation study, before applying the methods to our LT data in Section 4. We conduct 100 replicate trials for each simulation. For every trial, we generate new data on N individuals and then split the N individuals into training and test sets, with $0.8N$ individuals used for training and the remaining data used to assess performance. All three methods are used for each dataset.

In this section, we investigate: (1) whether wavelet variables have better performance in classification than the original variables; (2) which variables are more important in the tree; (3) which of the proposed methods perform better in different circumstances. Our criteria are prediction accuracy and the ability to correctly identify informative variables.

All computations were performed in R (R Core Team, 2014), using the packages rpart (Therneau et al., 2014) for constructing classification trees and waveslim (Whitcher, 2013) for wavelet decomposition.

3.1. Data generation

We generate panel data with two groups, comprising a total of $N = 300$ individuals. For each individual, there are 10 "time series" variables. Five of these variables (V_1–V_5) are informative, having different distributions in the two groups, while the remainder (V_6–V_{10}) are identically distributed across both groups and referred to as redundant variables. Details of the variables' models, distributions and parameters are shown in Table 1.

For each informative variable, the parameters of the models are chosen so that the first two moments are identical for the two groups. The five explanatory variables follow an AR process (V_1), sine models (V_2 and V_3), Poisson (V_4) and exponential (V_5) distributions, so we have both autocorrelated and independent variables. We independently generate $T^s_n \sim U(T_n/4, 3T_n/4)$ as a "change point" for each individual n, and for variables V_4 and V_5 observations before and after this point follow the

Table 1: Simulation variables and parameters. Variables V_1–V_5 are contaminated at rate θ by normally distributed noise which has the same mean and variance as the variable in question.

	variable name	distribution	parameters	
			group 1	group 2
Explanatory variables	V_1	AR(1)+$N(0,\sigma_2^2)$	$\alpha = 0.8$	$\alpha = 0.5$
			$\sigma_1^2 = 0.36$	$\sigma_1^2 = 0.75$
	V_2	sin+$N(0,\sigma_2^2)$	$2\sin(3t+5)$	$2\sin(4t+5)$
	V_3	sin+$N(0,\sigma_2^2)$	$2\sin(5t+6)$	$2\sin(5t+3)$
	V_4	Poisson	$\lambda_1 = 2$	$\lambda_1 = 2.5$
		+$N(0,\sigma_2^2)$	$\lambda_2 = 2.5$	$\lambda_2 = 2$
	V_5	exp (rate=λ)	$\lambda_1 = 1$	$\lambda_1 = 2$
		+$N(0,\sigma_2^2)$	$\lambda_2 = 2$	$\lambda_2 = 1$
Redundant variables	V_6	Poisson	$\lambda = 1$	
	V_7	Poisson	$\lambda = 2$	
	V_8	AR	$\alpha = 0.7$	
	V_9	MA	$\beta = 0.6$	
	V_{10}	exp	$\lambda = 8$	

same distribution but with different parameters. Noise is added to V_1–V_5 in two ways. Firstly, we add Gaussian white noise $\epsilon_t \sim N(0, \sigma_2^2)$, and we also contaminate the data by making random replacements at rate θ with $N(\mu, \sigma^2)$, where μ and σ^2 are the theoretical mean and variance of the variable in question. These data generation methods ensure that the marginal distribution for each explanatory variable between two groups is the same, while the joint distribution is different between two groups.

In order to assess the influence of noise levels and group balance on classification accuracy and selection of explanatory variables, we conduct simulations under different circumstances with noise level $0 \leqslant \sigma_2 \leqslant 20$, contamination rate $0.1 \leqslant \theta \leqslant 0.8$ and the number of individuals in group 1 ranging from 150 to 270, with the total number $N = 300$ fixed.

After generating our data, we carry out the wavelet transform on these variables, using the Haar wavelet. Then, we use the original and wavelet-transformed data for our simulation experiment. We conduct 100 replicate trials for each experiment.

3.2. Separate analysis for each explanatory variable

3.2.1. Classification accuracy

In order to tell which explanatory variable is most effective in classification, we built classification trees with only one informative explanatory variable at a time, replacing the other four informative variables with standard Gaussian white noise $N(0, \sigma_2 = 1)$. This provides a check that the CART methodology is correctly selecting informative variables while ignoring variables that contain no useful information. In each case, classification accuracy for the original variables on the test data is generally around 50%. However, Table 2 shows that, for wavelet variables, it is generally above 85% except for V_3, which is noticeably lower. In particular, variable V_2 is the most informative. We attribute this to the wavelet coefficients distinguishing the different frequencies of V_2 in the two groups. Method 3 is usually the best method due to the aggregation over time points effectively averaging out random variation, giving a cleaner picture of the differences between the groups.

3.2.2. Interpretation of scale choice

A further advantage of using wavelet-transformed data is the added insight which can sometimes be gained by considering which scales are used in the classification. In order to illustrate clearly, we simplify parameters by fixing $T_n = 768$ and $T_n^s = T_n/2 = 384$, and do not add white noise to the explanatory variables but for V_2–V_5, we still randomly replace 10% of generated observations with noise. Figures 1–3 show examples of the time series generated and plots of those wavelet-transformed variables which were most commonly selected as containing useful information by

Table 2: Classification accuracy when using wavelet-transformed version of each of the informative variables in isolation.

Method	Informative variable				
	V_1	V_2	V_3	V_4	V_5
1	86.83%	99.67%	53.67%	92.17%	97.17%
2	85.67%	100.00%	47.67%	93.00%	97.33%
3	100.00%	100.00%	94.33%	100.00%	100.00%

CART. We note that CART can easily detect differences in the mean level of a variable with a single split, and can also partially detect increased variance by two splits.

V_1 For V_1, the main variables chosen were s_8 (representing smoothing over a window of $2^8 = 256$ time points) and d_1 (the difference between successive observations). Recall that V_1 follows an AR(1) model with autoregressive parameter $\alpha = 0.8$ in group 1 and $\alpha = 0.5$ in group 2, so the short-term autocorrelation is substantially higher in group 1. Using the raw data does not access this information, but it is detected by the local averages in $V_1 s_8$ and local fluctuations in $V_1 d_1$.

V_2 For V_2, the frequency difference in the sine function is detected by both $V_2 s_1$ and $V_2 d_1$.

V_3 The sine function in the two groups differs only by a phase translation along the time axis. This is not easily recognized as it does not affect the autocorrelation or frequency characteristics which are encoded in the wavelet-transformed variables. Indeed, Methods 1 and 2 fail in this case.

Method 3 still works here, but the reasons are subtle and the improvement is in fact an artefact caused by the data length T_n not being a multiple of the cycle length of the sine wave. This means that changing the starting point of the cycle results in one part of the cycle being slightly over-represented, illustrated in Figure 2. This effect, though small, is picked up when the $V_3 s_8$ and $V_3 d_1$ variables are averaged over the full time series. Since this effect will change as the relationship between the cycle length and T_n changes, we would not expect the good performance of Method 3 to be relied upon for variables like V_3 in general.

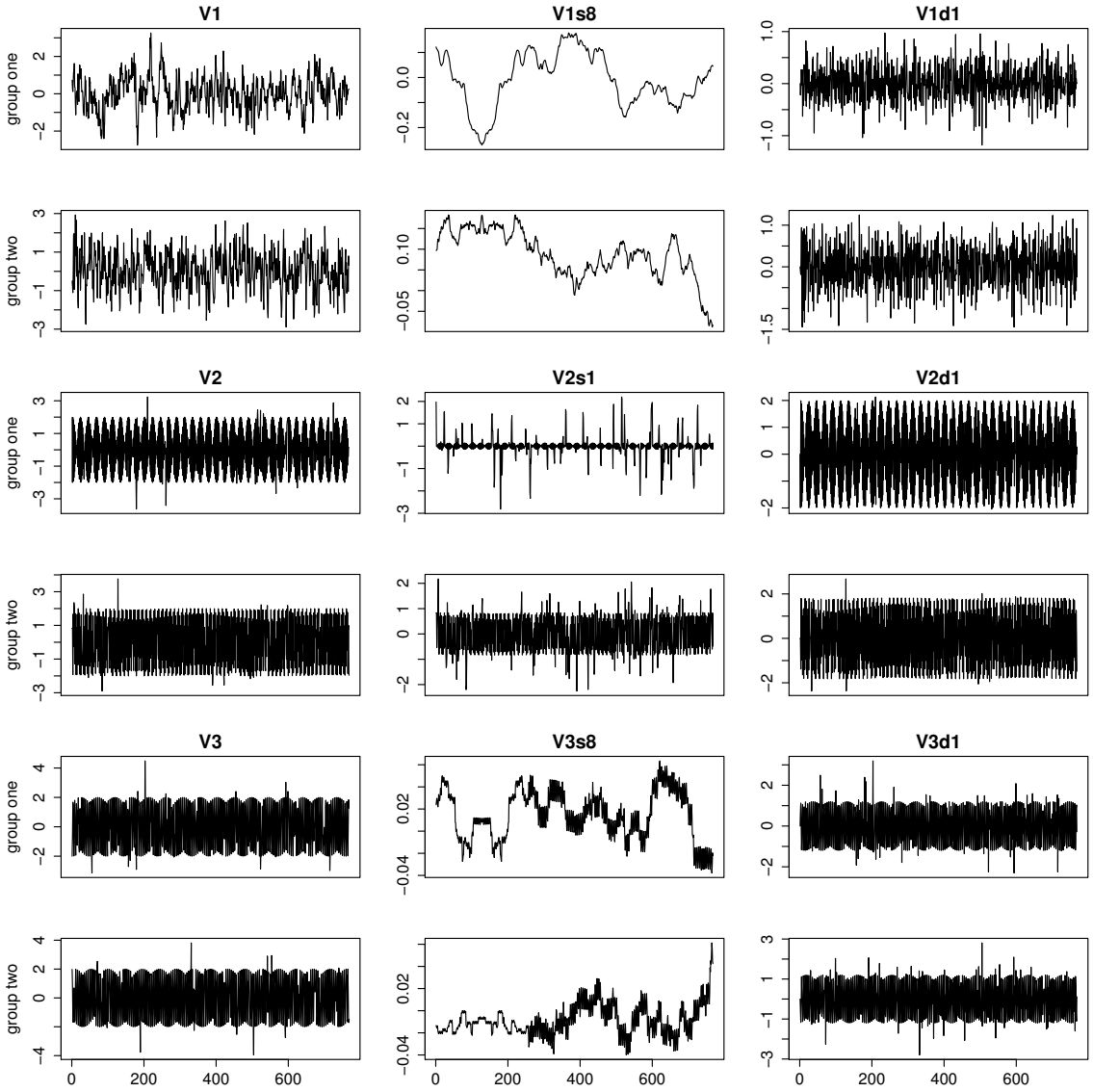

Figure 1: Wavelet transformed information for V_1–V_3 for individual one separately in group 1 and group 2 with 0.1 contamination rate and noise level 0, except V_1.

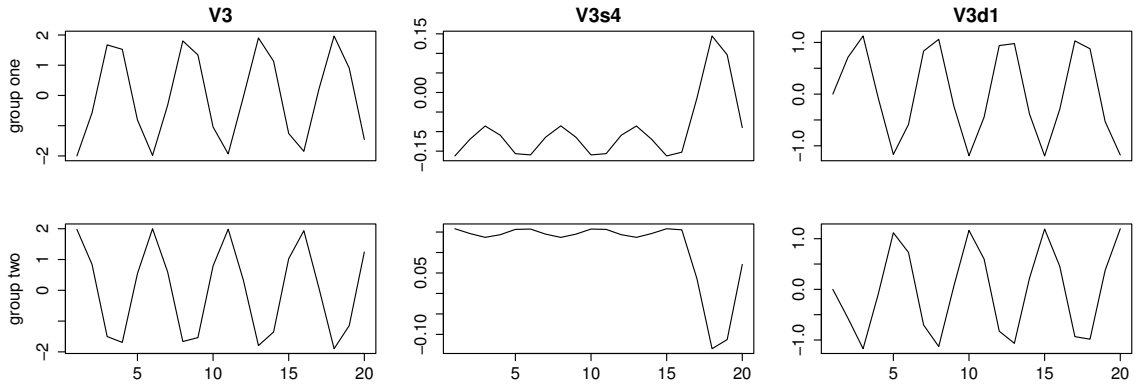

Figure 2: An example of V_3 for group 1 and group 2 with time length 20 and without noise added and contamination rate.

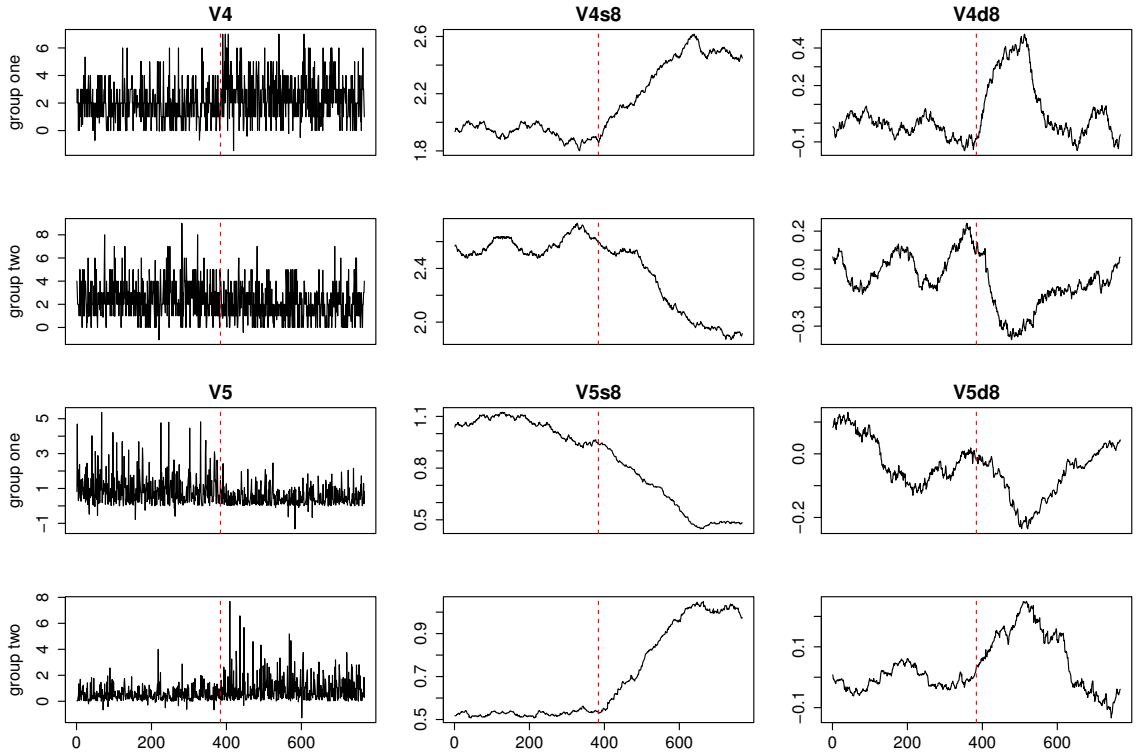

Figure 3: Wavelet transformed information for V_4–V_5 for individual one separately in group 1 and group 2 with 0.1 contamination rate and noise level 0.

V_4, V_5 These variables are each the same mixture when aggregated over time points, but differ in which parts of the signal they are slightly higher and lower. Visually, the difference is clear in the s_8 variables which form localized averages. This difference is lost when aggregated along the time axis, as happens with the original variables. However, the differences at scale 8 are extremely helpful here as they record larger positive (negative) values when there is an increase (decrease) in the local mean. In addition, the taking of localized means effectively averages out the white noise.

These differences could be detected from the original variables, but care would be needed to compute a summary statistic that would encode the differences between groups, especially if the location of the change point T_n^s is not known. Although the examples in Figure 3 have $T_n^s = T_n/2$ for simplicity, the wavelet-transformed variables will detect the presence of an increase or decrease in the localized means adaptively regardless of the best scale to average over or location of the change point.

3.3. Simulation with all explanatory variables included

3.3.1. Ideal circumstance

In ideal circumstances, we have noise level $\sigma_2 = 0$, a low contamination rate of $\theta = 0.1$ and equal group sizes. We also construct situations in which CART works for the original data, by adding an offset $\delta = 0.2$ to all observations of variables $V_1 - V_5$ in group 1, making the expectation of these variables higher in group 1.

Corresponding results in Table 3 show that using CART with the original data cannot distinguish the two groups using Methods 1 and 2, as it simply uses the default tree (classifying all individuals into the majority group). It is a little better when using Method 3, with a prediction accuracy of 36.7/60 and detecting explanatory variables V_1, V_3. However, using wavelet transformed data results in nearly 100% prediction accuracy. The explanatory variables and scales used are consistent with those in Figures 1–3. For Methods 1–2, V_2 is still the best explanatory variable, followed by V_5 (and V_1). For Method 3, V_1, V_5 and V_2 are all quite good.

When we use the increase in mean level, it is obvious that original data and wavelet-transformed data share identical accuracy. When explanatory variables have obvious mean-levels differences between two groups, wavelet-transformed variables have the same good performance as original data. In terms of variable choice, CART with original data generally chooses all the explanatory variables especially their means, and still selects redundant variables in some cases. However, CART with wavelet-transformed variables is more parsimonious while retaining excellent accuracy and is less likely to include redundant variables.

Table 3: Testing accuracy results with noise level $\sigma_2 = 0$, contamination rate $\theta = 0.1$ and equal group sizes of 150. Accuracy is the number of correctly classified individuals from a training set of 60, averaged over 100 replicate simulations. Entries – indicate that no splitting was done.

Method	Accuracy (/60, sd)		original		wavelet
	Original	Wavelet	variables*	redundant**	variables*
Offset $\delta = 0$					
1	30.0(0.00)	59.7(0.64)	–	–	V_2 V_5 V_1
2	30.0(0.00)	60.0(0.00)	–	–	V_2 V_5
3	36.7(3.90)	59.5(0.83)	V_1 V_3 (m sd)	yes	V_1 V_5 V_2
Offset $\delta = 0.2$					
1	59.8(0.46)	59.6(0.79)	V_5–V_1	yes	V_2 V_3
2	60.0(0.00)	59.9(0.34)	V_4 V_5 (m sd)	no	V_2 V_5 V_3
3	60.0(0.10)	59.7(0.59)	V_1–V_5 (m)	no	V_5 V_2

* Main variables in the first six important variables from CART.

** Whether redundant variables are used by CART.

No redundant variables were selected by CART using wavelet variables.

Table 4: Choice of variable, resolution level and wavelet or scaling coefficient when applying CART to wavelet-transformed simulated data.

Method	Variables (information)		
Offset $\delta = 0$			
1	V_2 (s_1, s_2, d_2)	V_5 (s_8, d_8, s_7)	V_1 (s_8)
2	V_2 $(d_1, d_2, s_1, s_2\,\mathrm{m\,sd})$	V_5 $(d_8, s_8\,\mathrm{m})$	
3	V_1 $(d_1, d_2\,\mathrm{sd})$	V_5 $(d_7, d_8\,\mathrm{m})$	V_2 $(d_1, d_2\,\mathrm{sd})$
Offset $\delta = 0.2$			
1	V_2 $(s_6$–$s_8)$	V_3 $(s_6$–$s_8)$	
2	V_2 $(s_8\,\mathrm{m\,sd})$	V_5 $(s_8\,\mathrm{m\,sd})$	V_3 $(s_8\,\mathrm{m\,sd})$
3	V_5 $(d_6$–$d_8, s_8\,\mathrm{m})$	V_2 $(s_1, s_2\,\mathrm{m})$	

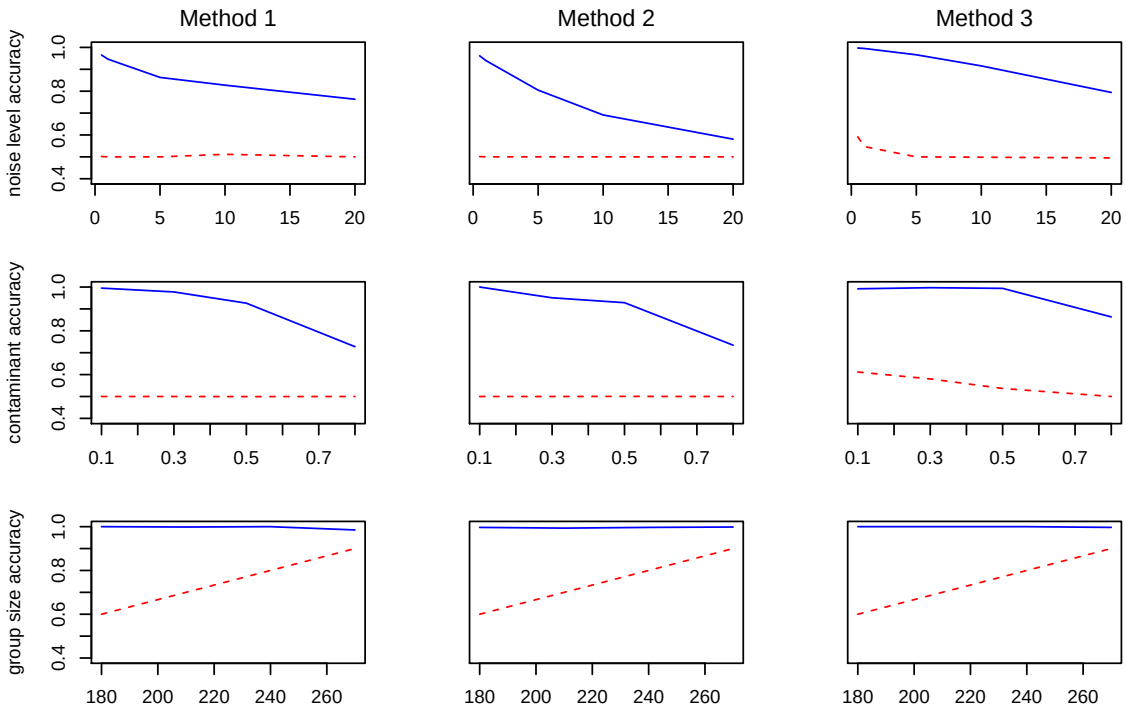

Figure 4: Testing accuracies results for real circumstances. Blue solid lines represent results for wavelet variables and red dash lines represent that for original variables. X-axis for the first row is noise level, for the middle row is contamination rate, for the last row is group 1 size.

3.3.2. Real circumstances

We now consider changes in noise level, contamination rate and group size balance. The corresponding results are shown in Figure 4. Each panel gives classification accuracy as the proportion of correctly classified individuals for both wavelet-transformed and original data (solid and dashed lines respectively) under a range of circumstances.

As one would expect, increasing noise or contamination levels reduces the accuracy of the methods using wavelet-transformed data, with Method 3 being least affected since the aggregation over time points before classification effectively averages out noise in the wavelet coefficients before conducting the classification procedures. The classification accuracy obtained using the original data is broadly unchanged, since classification was already essentially arbitrary in this case.

Making the groups more unbalanced leaves classification using wavelet-transformed data largely unchanged, while classification using the original data appears to improve since predicting all individuals to be from the dominant group becomes an

increasingly effective strategy.

3.4. Alternative wavelet transform functions

In the simulation, we have used the Haar wavelet basis defined in Equation (1). There are many other choices of wavelet basis available and we have repeated our analyses with minimum-bandwidth discrete-time wavelets with filter length 4 (mb4), Daubechies wavelets with filter length 4 (db4) and Least Asymmetric wavelets with filter length 8 (la8) in the R package waveslim. Full results are not included here, but they have shown that Haar is generally better than the others in most circumstances. Compared with la8, Haar is almost always better. When comparing Haar with mb4 and d4, Haar is better in all three methods with low noise level and low contaminant rate. When noise level and contaminant rate are high (5, 10, 20 and 0.5, 0.8 respectively), Haar is no longer the best in Methods 1 and 2 but still the best in Method 3. In most cases, Method 3 has the best performance. Therefore, due to good accuracy and the easier interpretation of the Haar wavelet, we recommend the Haar basis in practice.

4. Application to Liver Transplantation data

4.1. Data Description and Preprocessing

Liver Transplantation (LT) is a high-risk surgical treatment choice for patients suffering end-stage liver disease (Milan et al., 2016). Pre-operative treatment like beta-blockers may help reduce the surgical risk to some extent while also influencing the chance of surgical complications. For example, systolic dysfunction and low cardiac output with beta-blockers may compromise renal perfusion (Chirapongsathorn et al., 2016). So, if we can monitor variables like heart rate, systolic dysfunction and cardiac output effectively, then we may detect adverse effects earlier. We use these explanatory variables to classify patients as using or not using beta-blockers. In practice, a patient's beta-blocker use is known before surgery, but here we classify patients' into beta-blocker use to investigate which monitoring variables are considered informative in the classification.

Data on patients undergoing LT between September 2004 and December 2011 at St James' University Hospital, Leeds, UK, was recorded using LIDCO monitoring equipment (LIDCO, Cambridge, UK). The intraoperative monitoring variables recorded are shown in Table 5; for more details, see Milan et al. (2016). After removal from the data set of some individuals with poor-quality data, there are 90 patients who used beta-blocker (group 1) and 236 patients who did not (group 2). For each patient, the data consist of a multivariate time series of length one thousand to tens of thousands.

Table 5: Monitoring variables recorded in the liver transplant (LT) data set.

Abbreviation	Full name	Unit
CO	cardiac output	L/min
CI	cardiac index	L/min/m^2
SVR	systemic vascular resistance	dyne-s/cm^5
SVRI	systemic vascular resistance index	dyne-s/cm^5/m^2
Sys	systolic pressure	mm Hg
MAP	mean arterial pressure	mm Hg
Dia	diastolic pressure	mm Hg
SV	stroke volume	mL/beat
SVI	stroke volume index	mL/m^2/beat
HR	heart rate	beats/min

Since the number of patients in group 2 is around 2.6 times that in group 1, CART might be biased to predict new patients as being from group 2. This imbalance could be dealt with by using a cost matrix, by discarding data from the larger group, or by sampling replicate data from the smaller group. We chose the latter; after randomly sampling training and testing data from the entire data set, we triplicate the individuals from group 1 for training and testing data separately. There are then a total of 270 patients in group 1, relatively in balance with 236 patients in group 2. To investigate the robustness of our results to this procedure, we conduct the analysis twice, both with and without group size modification.

The data required considerable cleaning before classification could be attempted. There are some quite sharp increases and decreases, although variables like HR should not increase or decrease so suddenly as long as the patient is still alive. We assume that variables for each patient would not fluctuate sharply in a short time phase, and hence should remain within a limited range over a short time. Data points outside this range are regarded as outliers. There are also a non-trivial number of missing or impossible values. Firstly, we deal with data values outside the plausible range and we call this the *initial filter stage*. For the second stage, we will tackle data values which fluctuate sharply in a short time span and we call this the *secondary filter stage*.

Initial filter Since there are outliers, we use robust statistics for cleaning. Define

$$\text{mad}_{n,k} = \text{median}\left\{|A_{n,k,\cdot} - \text{median}(A_{n,k,\cdot})|\right\},$$

the median of the absolute deviations from the median. If $A_{n,k,t}$ is missing, infinite or zero, or satisfies

$$A_{n,k,t} \notin [\text{median}(A_{n,k,.}) - 5\,\text{mad}_{n,k},\ \text{median}(A_{n,k,.}) + 5\,\text{mad}_{n,k}],$$

then we carry the last observation forward and replace $A_{n,k,t}$ by $A_{n,k,t-1}$. If $t-1=0$, then we use the median of that variable. We use the previous value for replacement due to the presence of autocorrelation and since the previous value has already been defined as non-outlying.

Secondary filter In the secondary filter stage, we make the assumption that data values would not fluctuate sharply in a short time interval equal to 1/20 of the time series length. (Other time intervals were considered, but in practice for these data, intervals of $T_n/20$ worked well.) We define

$$Q^j_{n,k,p} = j^{th} \text{ decile of } \{A_{n,k,t_{i+1}}, A_{n,k,t_{i+2}}, \ldots, A_{n,k,t_{i+s}}\},$$

where $i = s(p-1)$, $s = T_n/20$ and $p = 1, 2, \ldots, 20$ refers to the p^{th} short time phase. With Q^1 and Q^9 as the first and ninth deciles and $d = Q^9 - Q^1$, we replace data values $A_{n,k,t} \notin [Q^1 - 1.5d,\ Q^9 + 1.5d]$ by $A_{n,k,t} = A_{n,k,t-1}$. If $t-1=0$, then $A_{n,k,t} = Q^5$.

After data cleaning for the whole data set, only a small proportion of the values (0.3% to 2% per variable) are changed. As an example, raw and cleaned CO data from patient 5 are shown in Figure 5.

4.2. Results

After data cleaning, we put the original and wavelet-transformed variables into our classification methods, randomly sampling 80% of the data for training and the remaining 20% for testing. To reduce sensitivity of observed classification accuracy to this sampling, we conducted 50 replicate trials for each method. The corresponding results are shown in Table 6.

Without group size adjustment, Methods 2 and 3 generally choose to split no variables and remain as default tree and Method 1 does worse than this, sometimes choosing group 1 as the main group during the time-point level tree construction process. Method 2 also has such cases, so that is why their standard deviations are high. Without these cases, they generally choose the default tree with accuracy around 45 to 46 and standard deviation around 1 and 2. These confirm that group size adjustment is needed in this case.

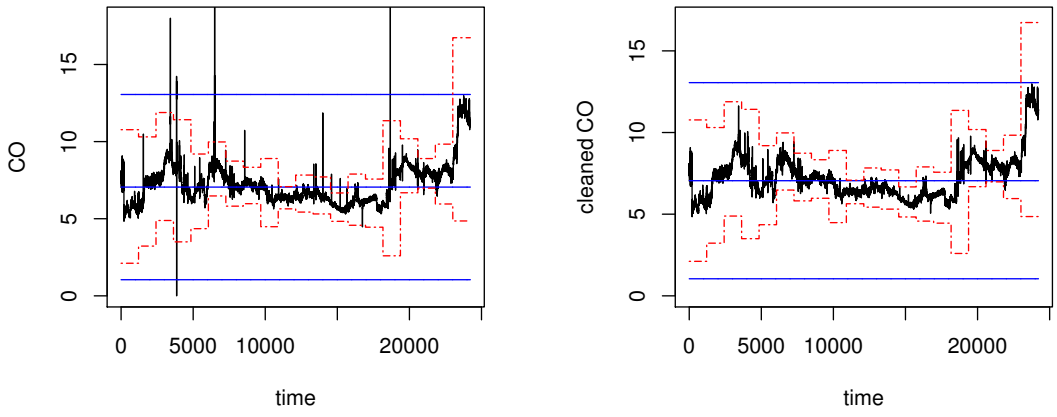

(a) original CO

(b) cleaned CO

Figure 5: Example of data cleaning for CO data from patient 1. Solid horizontal lines represent median and initial filter range, dashed lines represent secondary filter range.

After group size adjustment, individuals in group 1 account for 53.4% of all the individuals, approximately in balance with individuals in group 2. Student's t-test shows there are no significant differences between all three methods either for wavelet-transformed or for original data. However, accuracy from wavelet-transformed data is slightly higher in nearly all cases. This may be due to some variables' means in different groups being sufficiently different for decision rules using the original data to work well. When we come across data that has no significant mean difference, wavelet transform is highly recommended as its accuracy is significantly higher. Size adjustment initially seems to lower the accuracy, but it should be noted that with the balanced group sizes a default tree will now attain accuracy of 33/65. Without considering the time for wavelet transform, the computation time for Method 2 (around 7 hours per trial) is much longer than Method 3 (less than 1 second per trial). So, we find the best prediction of beta-blocker use to be achieved by using wavelet-transformed data in Method 3 with a size adjustment.

The main variables chosen are HR, SV, CO, SVR, SVI, and CI. CART based on wavelet-transformed data generally chooses smoothed variables on resolution level 9 or 10, effectively choosing to use moving-average versions of the original data. In this case, some variables have different means between the two groups (Milan et al., 2016), so CART based on original data works reasonably well, but the automatic

smoothing of the variables via the wavelet transform improves the classification. It also gives us the added interpretation that the optimal smoothing is done over a time window of 2^9–2^{10} heartbeats, approximately 5–17 minutes. This finding has clinical relevance. One of the main effects of beta-blockers is a slowing heart rate. A previous study that compared heart rates among a group of patients — both treated and not treated with beta-blockers — found a difference between two large groups with more than 10,000 measurements for each patient (Milan et al., 2016). Since clinical data during long surgical procedures were 'noisy', the complex statistics performed elicited the need for data smoothing. Wavelet-transformed variables have shown improved interpretation via consideration of which resolution scales are the most informative. This method can be applied to other 'noisy' databases in the future.

Table 6: Testing accuracy results for the LT data using Methods 1–3 with and without group size adjustment. The main variables listed are the first six important variables list output by CART.

Method	Accuracy (/65, sd)		Main variables*	
	original	wavelet	original	wavelet
Without size adjustment				
1	39.4(11.63)	45.16(6.09)	HR CO SV SVR CI SVRI SVI	HR CO SV CI s_9 s_{10}
2	44.46(7.07)	45.56(5.76)	–	–
3	46.7(1.16)	46.7(1.20)	–	–
With size adjustment				
1	39.2(4.53)	40.4(4.78)	HR CO SV SVR CI SVI	HR SV CO s_9 s_{10}
2	40.34(3.82)	41.94(6.32)	HR SV SVI m, sd	HRs_9 s_{10} (m, sd) SVIs_{10}(m,sd) Syss_{10}(m,sd) SVs_{10}(m,sd) Dias_{10}(m,sd)
3	38.82(2.86)	39.84(3.69)	HR m, SVR m, CI m, CO m, MAP m, SVI m SVRI m	HR s_1–s_8 m

5. Conclusions and discussion

Wavelets provide a basis for automatic feature extraction methods, allowing the classification technique (CART in our case) to select from localized means and differences over a range of scales. Compared to other feature extraction methods, the initial process is *not* dimension reduction. Feature extraction methods such as principal component analysis (Asavaskulkeit and Jitapunkul, 2009), Locality sensitive hashing (Datar et al., 2004), and manifold learning (Costa and Hero, 2004; Nie et al., 2010), all aim to reduce the number of explanatory variables whilst using wavelet-transformed variables actually *increase* the dimension by transforming original variable into detail and smoothed coefficients on different resolution levels. This can reveal hidden information which is not easy for classification trees to find using only the original data. This does mean that wavelet transformation of the data is more suitable for experiments without an excessive number of predictors, otherwise a further variable reduction step will be required and this will increase the computational burden (Mazloom and Ayat, 2008; Chitaliya and Trivedi, 2010; Li and Wen, 2014).

CART, as a decision tree method, can be seen as a variable reduction method since it chooses the "best" variable to split on in each step. Compared to methods like ANN (Rowley et al., 1998), SVM (You et al., 2014) and LASSO (Roberts and Nowak, 2014), its main advantage is its ease of interpretation, although it might not achieve the same accuracy as other methods. When applying CART to wavelet-transformed data, the disadvantages of using the wavelet transform are mitigated since CART carries out a dimension reduction function. By learning which wavelet-transformed variables are more effective, we can also gain the added interpretation of which scales are important.

Compared to other feature extraction methods, the wavelet transform has its own advantages. It helps discover information hidden by noise that can not be achieved by other methods which do not provide information decomposition across different scales for one single variable. In our simulation, we have shown the effectiveness of wavelet-transformed data in CART classification where the key features of interest are changes in autocorrelation or frequency structures (our variables V_1 and V_2), or relatively small changes in mean level which occur at unknown times and are hidden by considerable noise (V_4 and V_5).

The scaling function we use in wavelet decomposition is the Haar wavelet, the simplest case of the compactly-supported wavelets described by Daubechies (1992). In our experience, the Haar wavelet tends to have equal or better accuracy than other choices of wavelet and has the benefit or easier interpretation. For data whose expectation and variance have some connection, such as our Poisson and exponen-

tially distributed V_4 and V_5, we might consider using the Haar-Fisz wavelet transform (Fryzlewicz and Nason, 2004). Since, in real situations, we will usually not know the distribution of the time series, we generally use the Haar wavelet which is a robust all-purpose selection that allows for easy interpretation compared to more complicated wavelet bases.

We set out to produce individual-level predictions from panel data, where simple application of CART produces time-point level predictions. Comparison of the different methods we used has shown that methods which perform at least some aggregation before prediction have improved performance over a naive approach of predicting at each time point and using a simple voting mechanism to aggregate these predictions. Additionally, aggregation before classification (Method 3) is computationally quite fast in comparison to Methods 1 and 2. So, overall, we recommend Method 3 with wavelet transformed data.

Acknowledgement

Xin Zhao is grateful for the financial support of the China Scholarship Council (CSC) during this research.

References

Alickovic, E. and Subasi, A. (2016). Medical decision support system for diagnosis of heart arrhythmia using DWT and random forests classifier, *Journal of Medical Systems* **40**(4): 1–12.

Asavaskulkeit, K. and Jitapunkul, S. (2009). The color face hallucination with the linear regression model and MPCA in HSV space, *2009 16th International Conference on Systems, Signals and Image Processing*, IEEE, pp. 1–4.

Breiman, L., Friedman, J., Stone, C. J. and Olshen, R. A. (1984). *Classification and Regression Trees*, Wadsworth, Belmont.

Chirapongsathorn, S., Valentin, N., Alahdab, F., Krittanawong, C., Erwin, P. J., Murad, M. H. and Kamath, P. S. (2016). Nonselective β-blockers and survival in patients with cirrhosis and ascites: A systematic review and meta-analysis, *Clinical Gastroenterology and Hepatology* .

Chitaliya, N. G. and Trivedi, A. (2010). Feature extraction using wavelet-pca and neural network for application of object classification & face recognition, *Computer Engineering and Applications (ICCEA), 2010 Second International Conference on*, Vol. 1, IEEE, pp. 510–514.

Coifman, R. R. and Donoho, D. L. (1995). Translation-invariant de-noising, *in* A. Antoniadis and G. Oppenheim (eds), *Wavelets and Statistics*, Vol. 103 of *Lecture Notes in Statistics*, Springer-Verlag, New York, pp. 125–150.

Costa, J. A. and Hero, A. O. (2004). Geodesic entropic graphs for dimension and entropy estimation in manifold learning, *IEEE Transactions on Signal Processing* **52**(8): 2210–2221.

Datar, M., Immorlica, N., Indyk, P. and Mirrokni, V. S. (2004). Locality-sensitive hashing scheme based on p-stable distributions, *Proceedings of the Twentieth Annual Symposium on Computational Geometry*, ACM, pp. 253–262.

Daubechies, I. (1992). *Ten Lectures on Wavelets*, SIAM, Philadelphia.

Donoho, D. L. and Johnstone, J. M. (1994). Ideal spatial adaptation by wavelet shrinkage, *Biometrika* **81**(3): 425–455.

Fryzlewicz, P. and Nason, G. P. (2004). A Haar-Fisz algorithm for Poisson intensity estimation, *Journal of Computational and Graphical Statistics* **13**(3): 621–638.

Gokgoz, E. and Subasi, A. (2015). Comparison of decision tree algorithms for EMG signal classification using DWT, *Biomedical Signal Processing and Control* **18**: 138–144.

Li, S. and Wen, J. (2014). A model-based fault detection and diagnostic methodology based on PCA method and wavelet transform, *Energy and Buildings* **68**: 63–71.

Maharaj, E. A. and Alonso, A. M. (2007). Discrimination of locally stationary time series using wavelets, *Computational Statistics & Data Analysis* **52**: 879–895.

Maharaj, E. A. and Alonso, A. M. (2014). Discriminant analysis of multivariate time series: Application to diagnosis based on ecg signal, *Computational Statistics & Data Analysis* **70**: 67–87.

Mazloom, M. and Ayat, S. (2008). Combinational method for face recognition: wavelet, PCA and ANN, *Digital Image Computing: Techniques and Applications (DICTA), 2008*, IEEE, pp. 90–95.

Milan, Z., Taylor, C., Armstrong, D., Davies, P., Roberts, S., Rupnik, B. and Suddle, A. (2016). Does preoperative beta-blocker use influence intraoperative hemodynamic profile and post-operative course of liver transplantation?, *Transplantation Proceedings* **48**(1): 111–115.

Nason, G. P. and Silverman, B. W. (1995). The stationary wavelet transform and some statistical applications, *in* A. Antoniadis and G. Oppenheim (eds), *Wavelets and Statistics*, Vol. 103 of *Lecture Notes in Statistics*, Springer-Verlag, New York, pp. 281–300.

Nie, F., Xu, D., Tsang, I. W.-H. and Zhang, C. (2010). Flexible manifold embedding: A framework for semi-supervised and unsupervised dimension reduction, *IEEE Transactions on Image Processing* **19**(7): 1921–1932.

Percival, D. B. and Walden, A. T. (2000). *Wavelet Methods for Time Series Analysis*, Cambridge University Press, Cambridge.

R Core Team (2014). *R: A Language and Environment for Statistical Computing*, R Foundation for Statistical Computing, Vienna, Austria.
URL: *http://www.R-project.org/*

Roberts, S. and Nowak, G. (2014). Stabilizing the lasso against cross-validation variability, *Computational Statistics & Data Analysis* **70**: 198–211.

Rowley, H. A., Baluja, S. and Kanade, T. (1998). Neural network-based face detection, *IEEE Transactions on Pattern Analysis & Machine Intelligence* **20**(1): 23–38.

Therneau, T., Atkinson, B. and Ripley, B. (2014). *rpart: Recursive Partitioning and Regression Trees*. R package version 4.1-8.
URL: *http://CRAN.R-project.org/package=rpart*

Upadhyaya, S. and Mohanty, S. (2016). Localization and classification of power quality disturbances using maximal overlap discrete wavelet transform and data mining based classifiers, *IFAC-PapersOnLine* **49**(1): 437–442.

Whitcher, B. (2013). *waveslim: Basic wavelet routines for one-, two- and three-dimensional signal processing*. R package version 1.7.3.
URL: *http://CRAN.R-project.org/package=waveslim*

You, W., Yang, Z. and Ji, G. (2014). Feature selection for high-dimensional multi-category data using PLS-based local recursive feature elimination, *Expert Systems with Applications* **41**(4): 1463–1475.

Zhang, Y., Wang, S., Phillips, P., Dong, Z., Ji, G. and Yang, J. (2015). Detection of Alzheimer's disease and mild cognitive impairment based on structural volumetric MR images using 3D-DWT and WTA-KSVM trained by PSOTVAC, *Biomedical Signal Processing and Control* **21**: 58–73.